Open Access Research Journal of
Engineering and Technology
Journals home page: https://oarjpublication/journals/oarjet/
ISSN: 2783-0128 (Online)

OARJ OPEN ACCESS RESEARCH JOURNALS

(RESEARCH ARTICLE)

Check for updates

MICROSTRUCTURAL CHARACTERIZATION AND MECHANICAL PROPERTIES OF AA6061 ALUMINIUM MATRIX COMPOSITES REINFORCED WITH EUTALLOY® BRONZOCHROM 10185 AND COCONUT SHELL ASH

Adekunle Adetayo YEKINNI [1,*], Lukman Aremu ANIMASHAUN [1], Kasali Aderinmoye ADEDEJI [2], Kabiru Alani OLAIYA [1], Taiwo Olugbenga RABIU [1] and Sherif Babatunde LAMIDI [1]

[1] Department of Mechanical Engineering, Lagos State University of Science and Technology, Ikorodu, Lagos.
[2] Department of Mechanical Engineering, Lagos State University, Ojo, Lagos.
* Corresponding Author

ORCID Details
Adekunle Adetayo YEKINNI: https://orcid.org/0000-0003-3053-2297
Lukman Aremu ANIMASHAUN: https://orcid.org/0000-0001-8301-5889
Kasali Aderinmoye ADEDEJI: https://orcid.org/0000-0002-0311-2126
Kabiru Alani OLAIYA: https://orcid.org/0000-0002-9453-3320
Sherif Babatunde LAMIDI: https://orcid.org/0000-0002-3417-969X

Open Access Research Journal of Engineering and Technology, 2026, 11(02), 064–075

Publication history: Received on 14 October 2026; revised on 23 November 2026; accepted on 25 November 2026

Article DOI: https://doi.org/10.53022/oarjet.2026.11.2.0077

Copyright © 2026 Author(s) retain the copyright of this article. This article is published under the terms of the Creative Commons Attribution License 4.0

ABSTRACT

The necessity for lightweight, robust, and environmentally sustainable materials has sparked interest in hybrid aluminium matrix composites that utilize both metallic and agricultural-waste-derived reinforcements. This research examined the microstructure and mechanical properties of AA6061 composites hybrid-reinforced with Eutalloy® BronzoChrom 10185, a commercially available nickel-based Ni–B–Si alloy, and coconut shell ash (CSA), fabricated through stir casting. One unreinforced alloy and four hybrid formulations containing 2–10 wt.% BronzoChrom 10185 and 2–8 wt.% CSA were analysed using scanning electron microscopy (SEM), tensile testing, and Vickers microhardness measurements. SEM observations revealed variations in surface morphology, including localized particle agglomeration and void-like features at the highest combined reinforcement content. The ultimate tensile strength and hardness increased with increasing combined reinforcement content, whereas elongation decreased. Sample 4A attained a UTS of 143.92 MPa and a hardness of 75.8 HV, representing increases of 21.50% and 22.65%, respectively, compared with unreinforced AA6061. These findings identify Sample 4A, containing 10 wt.% BronzoChrom 10185 and 8 wt.% CSA, as the best-performing composition among those investigated in terms of measured tensile strength and hardness. The results demonstrate the potential of combining a nickel-based alloy with coconut shell ash to enhance the strength and hardness of AA6061, while highlighting the need to balance these improvements against the associated reduction in ductility. This hybrid reinforcement approach also offers a potential pathway for incorporating agricultural-waste-derived material into aluminium composites for applications where increased hardness and strength are desirable.

Keywords: AA6061 aluminium alloy; Eutalloy® BronzoChrom 10185; Nickel Based Ni–B–Si alloy; Coconut shell ash; Hybrid aluminium matrix composite; Stir casting; SEM; Mechanical characteristics.

1 INTRODUCTION

Aluminium based composites combine the low density and corrosion resistance of aluminium alloys with the improved mechanical and functional qualities of the reinforcing phases. The AA6061 alloy is particularly attractive for structural applications due to its good strength-to-weight ratio, heat-treatability, corrosion resistance and ease of fabrication. Recent studies have shown that appropriate selection and processing of reinforcements can improve the mechanical and tribological performance of aluminium matrix composites, including AA6061-based systems [1]-[3].

Hybrid reinforcement with two or more reinforcing types provides an efficient route to customize the microstructure and mechanical response of aluminium matrix composites [4]. The use of metallic, ceramic and waste generated reinforcements might affect the distribution of particles, the bonding between matrix and particles, the hardness and strength. For example, Hatti [1] reported enhanced mechanical behaviour of aluminium based green metal matrix composites augmented with silicon carbide and agricultural waste produced eggshell powder. Hybrid reinforcement of Al6061 with metallic and non-metallic constituents has been investigated as a means of tailoring microstructure and mechanical properties [5]. Prabhu [2] observed the effect of coconut shell ash (CSA) and red mud on physical and mechanical properties of AA6061, and Samantra [3] showed the potential of CSA to enhance mechanical and wear properties. Tang [6] also demonstrated the increase in the ductility without sacrificing the strength due to the use of hybrid SiC and stainless-steel reinforcement in 6061 Al. The stainless-steel particles assisted in load transfer and strain distribution. These results indicate the potential of complementary reinforcements for balancing the mechanical properties although the reinforcement combinations are different from the present system.

Materials generated from agro-waste have gained increasing interest as sustainable reinforcing materials, as they can alleviate waste-disposal difficulties and provide low-cost particle reinforcement. CSA is particularly attractive, as the mineral ingredients of CSA contain significant oxide phases, including silica-rich compounds, that can be used for particle strengthening and waste valorisation. Yekinni [7] showed that it is possible to produce hybrid recycled-aluminium composites with CSA and graphite by using a stir casting. Jaga Kumar [8] demonstrated an enhancement in the mechanical and tribological properties of aluminium composites supplemented with CSA and graphene, in terms of hardness and tensile strength. The changes in density and impact behaviour were also documented. Tejyan [9] studied the CSA- and cow-dung-ash-reinforced composites made by stir casting for AA6061 and reported variations in hardness, impact strength and tensile characteristics with reinforcement content. Microstructural evidence of reinforcement incorporation in AA6061/CSA/graphene composites was also reported by [8]. Later, the combined influence of graphene and CSA on Al6061 mechanical characteristics was investigated [10].

The reinforcing capability of coconut shell ash (CSA) extends beyond AA6061 aluminium alloys to other aluminium-based matrices. Poornesh et al. [11] reported that recycled CSA can enhance the tensile strength of a hypereutectic Al–Si alloy, with reinforcement composition, melting temperature, and stirring speed having significant effects on the resulting tensile properties. These findings indicate that CSA should not be regarded merely as a passive filler; rather, its effectiveness as a reinforcement depends on factors such as its addition level, particle characteristics, dispersion within the matrix, and interfacial interaction with the aluminium alloy [9], [11].

Another approach to improving the strength and hardness of aluminium matrix composites involves enhanced load transfer and restriction of plastic deformation through the incorporation of metallic reinforcements. Kumar and Bairwa [12] reported that the addition of Ni and Cr reinforcements to Al6061-based hybrid metal matrix composites improved their mechanical properties, with the improvements attributed in part to the resulting microstructural development. Similarly, Beldar and Kumavat [13] reported improvements in the strength and hardness of Al6061 composites containing Ni- and Cr-based reinforcements at appropriate compositions. These findings provide a basis for investigating the role of nickel-containing metallic reinforcements in AA6061. However, the reinforcement used in the present investigation differs from the elemental Ni and Cr reinforcements considered in these studies. In the present work, a commercial nickel-based Ni–B–Si alloy powder is employed as the metallic reinforcement rather than elemental nickel or chromium.

Eutalloy® BronzoChrom 10185 is a commercial nickel alloy powder for applications needing wear and corrosion resistance. According to the technical literature of the producer, BronzoChrom 10185 is a nickel-based alloy with boron and silicon, with nickel as the balance (Castolin Eutectic, n.d.). For this reason, it is referred to throughout this study as Eutalloy® BronzoChrom 10185, a commercial nickel-based Ni–B–Si alloy. This distinction is essential because if the chromium discovered by EDS is present, it is an empirically determined minor constituent and should not be used to redefine the commercial alloy label.

The use of BronzoChrom 10185 and CSA particles dispersed in an AA6061 matrix provides the possibility to study the interaction between a metallic nickel-based reinforcement and an oxide-rich agro-waste reinforcement. The hybrid system can promote strengthening by particle dispersion, interfacial load transfer, restriction of dislocation motion and

modification of microstructural development. Similar effects of nickel reinforcement have been reported in other aluminium-alloy matrix composites [14]-[15]. The results of Ni- and Cr-containing AA6061 composites provide evidence of the potential contribution of metallic particulate reinforcement, while studies involving CSA demonstrate the effectiveness of agro-waste-derived particles in modifying the mechanical and microstructural response of aluminium composites [3], [8], [9], [12], [13]. However, these investigations do not represent the chemistry or behaviour of BronzoChrom 10185 directly. The interaction of this commercial Ni–B–Si alloy with CSA in AA6061 is not well-established.

Composites of AA6061 with CSA, graphene, Ni or Cr have been studied however the combined usage of CSA and a commercial nickel-based Ni–B–Si alloy has not received much attention. Previous research has mainly investigated CSA with ceramic or carbon-based phases or Ni- and Cr-containing reinforcements independently [2], [8], [12], [13]. Also, the CSA/graphite study of [7] demonstrated the possibility of coupling CSA with another particle reinforcement in recycled aluminium, although it does not tackle the AA6061/BronzoChrom hybrid system. Thus, the link between phase composition, microstructure formation and mechanical performance in the AA6061/BronzoChrom 10185–CSA system is still badly understood.

Stir casting is a convenient and cost-effective method for manufacturing particle aluminium matrix composites and has been successfully used with CSA- and other particulate reinforced aluminium systems [7], [8], [9], [12], [16]. However, the resulting properties might be influenced by the distribution of reinforcements, agglomeration, porosity, wetting and interface contact between matrix and particles. Complementary characterisation is thus required to determine the link between processing, phase constitution, microstructure and mechanical response. X-ray diffraction (XRD) is used to characterize main crystalline phases, whilst scanning electron microscopy (SEM) and energy-dispersive X-ray spectroscopy (EDS) are used to study morphology, particle distribution and chemical content. The related mechanical reaction is quantified by tensile and hardness tests. These integrated characterizations have been employed in the current sustainable and hybrid aluminium composite research [1]-[3].

Therefore, the present work aims to fill the research gap by producing the AA6061 hybrid composites with different ratios of Eutalloy ® BronzoChrom 10185 and CSA by stir casting and assessing their phase constitution, microstructure and mechanical behaviour. The main contribution is the invention and characterisation of a hybrid reinforcing system BronzoChrom 10185-CSA for the AA6061 alloy. The effect of increasing combined reinforcement content on the crystalline phases, microstructural development, ultimate tensile strength, elongation and Vickers hardness is discussed. The work aims at clarifying the links between reinforcing content, phase constitution, microstructural development and mechanical performance in the examined composition range by integrating SEM and mechanical characterization.

2 MATERIALS AND METHODS

2.1 Materials

The matrix material was decided to be AA6061 aluminium alloy because of its low density, corrosion resistance and weldability, as well as strong mechanical performance, which make it suited for structural applications. The metallic reinforcement was a commercial nickel-based hard face alloy (Figure 1a) Eutalloy® BronzoChrom 10185, containing Ni, B, Si and other alloying ingredients, which is hereafter referred to as the Ni–B–Si alloy for brevity. The sustainable agro-waste-based reinforcement, coconut shell ash (CSA), was used to offer a supplementary particulate phase to the metallic Ni–B–Si alloy.

2.2 Preparation of Coconut Shell Ash

The collected coconut shells were washed completely, air dried and calcined in a muffle furnace at 450 °C for 4 h. The calcined ash was then crushed and ground to a fine powder, sieved and stored in sealed containers to minimize moisture uptake before use (Figure 1b). Calcination assists in removing volatile constituents and can modify the oxide-rich composition of agro-waste ash, potentially improving its suitability as particulate reinforcement [11].

2.3 Composite Formulation

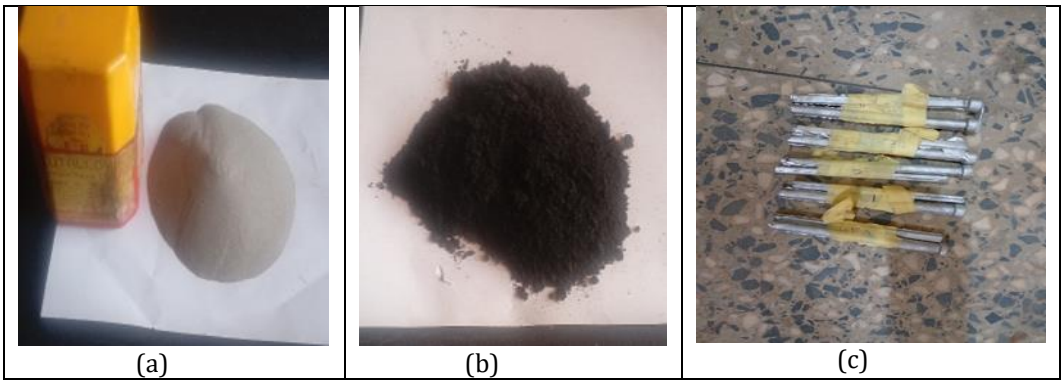
Five compositions were prepared as shown in Table 1: one unreinforced control and four hybrid composites. The microstructure and mechanical properties of AA6061 were investigated by increasing the reinforcement content step by step, using Ni–B–Si alloy powder and CSA as reinforcements.

Table 1: Composition of Developed Hybrid Composites

Sample ID	AA6061 (wt.%)	CSA (wt.%)	Ni-B-Si based alloy powder (wt.%)
0A	100	0	0
1A	96	2	2
2A	90	4	6
3A	86	6	8
4A	82	8	10

2.4 Stir casting preparation

The AA6061 was melted at a temperature of around 760 °C in a graphite crucible. To lower the temperature gradients and facilitate the integration of the molten alloy, the Ni–B–Si based alloy powder and CSA particles were pre-heated at 350 °C for 1 h. The heated reinforcements were gradually added to the molten alloy and mechanically agitated for 10 min at 500 rpm. After stirring, the slurry was cast into steel moulds and allowed to cool at room temperature before machining for characterisation (Figure 1c). Stir casting is still a relatively cost-effective and scalable method for creating particulate aluminium matrix composites [1], [2].



(a) (b) (c)

Figure 1: (a) Eutalloy@BronzoChrom 10185 Powder (Ni-B-Si based alloy) (b) Coconut shell ash (c) Casting of control sample and four composites

2.5 Characterization by SEM

Scanning electron microscopy (SEM) was conducted using a JEOL JSM-5900LV microscope and elemental analysis was undertaken using an Oxford INCA™ energy-dispersive X-ray spectroscopy instrument. The analyses were applied to investigate the microstructural morphology.

2.6 Tensile test

Tensile testing was carried out according to ASTM E8/E8M on an Instron 3369 universal testing equipment with extensometer. The crosshead speed was maintained at 2mm/min. For each composition (0A–4A) one tensile specimen was evaluated. So, the reported tensile characteristics are the reaction of the individual specimens tested and not an estimate of specimen-to-specimen variability or statistical uncertainty. This constraint should be taken into account when analysing differences in tensile qualities between the compositions.

2.7 Vickers Microhardness Test

Vickers microhardness measurements were made according to ASTM E384 on a LECO AT700 microhardness tester. Four indentations were produced on each of the samples at different points using a diamond indenter. The quoted Vickers hardness value is the average of four measurements for each composition.

3 RESULTS AND DISCUSSIONS

3.1 Chemical Composition of AA6061 Aluminium Alloy, Nickel Based Ni-B-Si Powder and Coconut Shell Ash

As can be seen from Table 2, Eutalloy BronzoChrom 10185 is a nickel-based Ni–B–Si alloy with Ni as the balance, about 3.0 wt.% Si and 2.5 wt.% B and only minimal Cr and Fe (≤0.5 wt.% each). The Si and B contents are related with the hardening and supposed to add to the strength and hardness of the composite.

The results in Table 3 indicate that the coconut shell ash (CSA) mostly consists of SiO_2 with substantial levels of MgO, Al_2O_3 and FeO. Its high silica and oxide levels indicate its potential as a ceramic particle reinforcement in AA6061 that contributes to hardness and resistance to plastic deformation (Yekinni et al., 2020).

The CSA and Ni–B–Si alloy offer complimentary oxide/ceramic and metallic hard-phase reinforcing effects to the AA6061 matrix.

Table 2: Chemical composition (wt.%) of Eutalloy BronzoChrom 10185

Ni	Si	B	Cr	Fe	C
Balance	3.0	2.5	≤0.5	≤0.5	≤0.1

Source: Castolin Eutectic [17]

Table 3: Chemical composition (wt.%) of coconut shell ash produced by burning at 450°C.

SiO_2	Al_2O_3	FeO	MgO	MnO	K_2O	Na_2O	ZnO	LOI
48.213	15.234	12.673	16.574	0.625	1.811	0.892	0.472	3.206

Source: Yekinni [7]

3.2 SEM-Based Microstructural Characterization and Image Analysis

Figures 2(a–e) present the scanning electron microscopy (SEM) micrographs of unreinforced AA6061 and the hybrid composites containing different proportions of coconut shell ash (CSA) and Eutalloy® BronzoChrom 10185, a nickel-based Ni–B–Si alloy. The micrographs were examined to compare the surface morphology and apparent distribution of microstructural features across the investigated compositions. The observations provide a qualitative basis for discussing changes associated with reinforcement incorporation, although definitive identification of individual phases, reinforcement particles, grain boundaries and pores requires complementary characterization or validated image analysis.

The SEM micrograph of unreinforced AA6061 (Sample 0A), shown in Figure 2(a), exhibits relatively large polygonal regions separated by prominent boundaries, together with localized variations in surface contrast. These features provide a reference for assessing the morphological changes observed in the reinforced samples. The contrasting regions may be associated with variations in surface topography or differences in the underlying microstructure; however, their identities cannot be established from SEM morphology alone. Unlike the reinforced composites, sample 0A contains no deliberately added CSA or BronzoChrom 10185 reinforcement.

Figure 2(b) shows the microstructure of Sample 1A, containing 2 wt.% CSA and 2 wt.% BronzoChrom 10185. Compared with the unreinforced alloy, the micrograph exhibits a more intricate arrangement of bright and dark features, including numerous rounded or elongated dark regions surrounded by brighter boundaries. These features indicate a change in the observed surface morphology following reinforcement incorporation. Although some regions appear reasonably interconnected, the image alone does not establish the identity or distribution uniformity of individual reinforcement particles or confirm the quality of matrix–particle bonding. The dark regions also cannot be assigned unequivocally to pores because surface depressions, matrix contrast and other features may produce similar appearances.

The SEM micrograph of Sample 2A, containing 4 wt.% CSA and 6 wt.% BronzoChrom 10185, is presented in Figure 2(c). The image displays relatively large dark regions separated by bright, irregular boundaries, with localized concentrations of bright features. The morphology differs from that of Samples 0A and 1A, suggesting that the combined reinforcement system is associated with changes in the observed surface features. However, the apparent differences do not independently establish grain refinement, reinforcement agglomeration or the extent of interfacial bonding. Quantitative grain-size measurements and reliable identification of the relevant phases would be required to substantiate such interpretations.

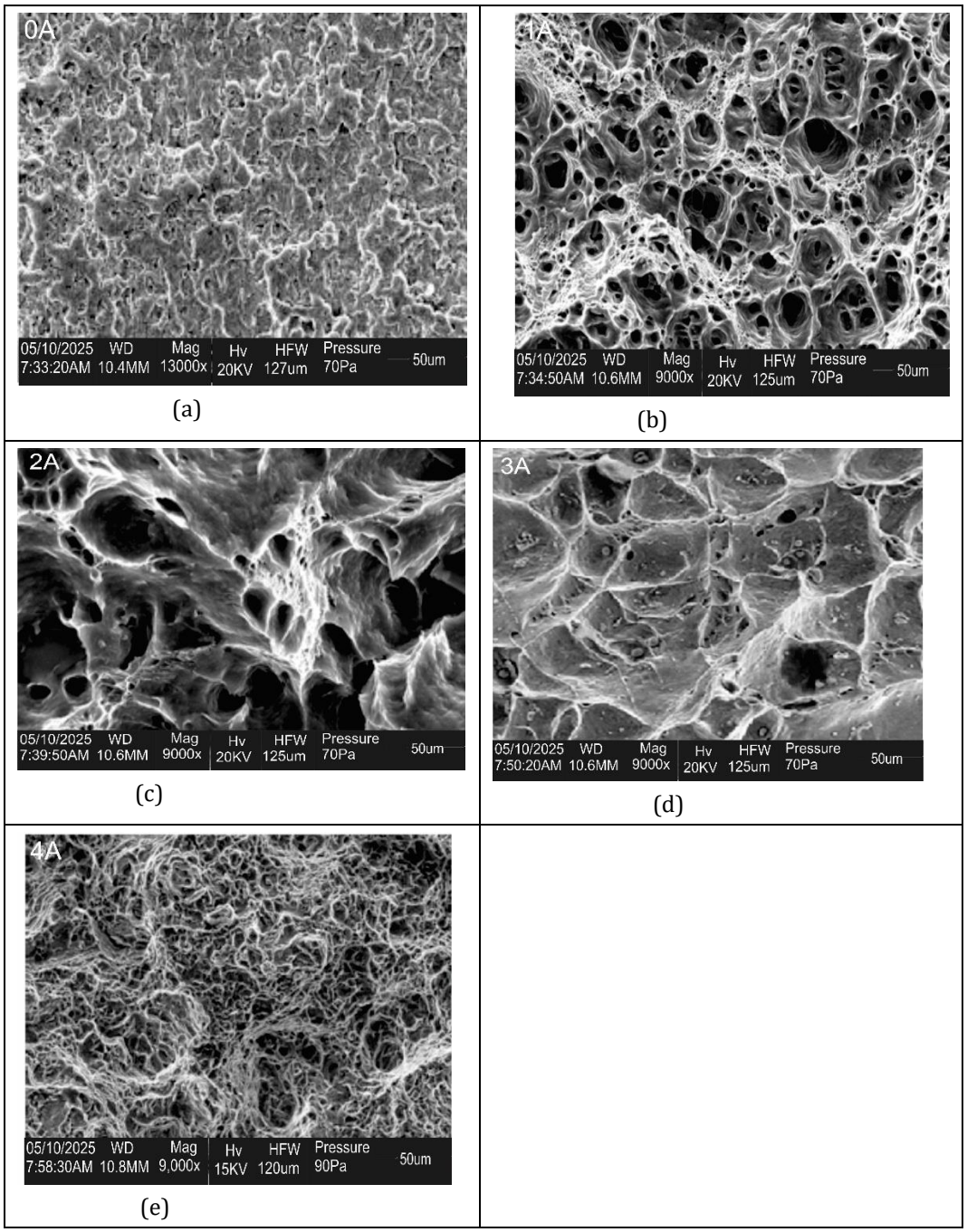


Figure 2: SEM of (a) unreinforced AA 6061 Alloy. (b) AA 6061 reinforced with 2 wt.% coconut shell ash (CSA) and 2 wt.% Eutalloy® BronzoChrom 10185 (Ni–B–Si alloy) (c) AA 6061 reinforced with 4 wt.% coconut shell ash (CSA) and 6 wt.% Eutalloy® BronzoChrom 10185 (Ni–B–Si alloy) (d) AA 6061 reinforced with 6 wt.% coconut shell ash (CSA) and 8 wt.% Eutalloy® BronzoChrom 10185 (Ni–B–Si alloy) (e) AA6061 reinforced with 8 wt.% coconut shell ash (CSA) and 10 wt.% Eutalloy® BronzoChrom 10185 (Ni–B–Si alloy respectively

Figure 2(d) presents the micrograph of Sample 3A, containing 6 wt.% CSA and 8 wt.% BronzoChrom 10185. Polygonal regions remain visible, while the boundaries and surrounding features exhibit variations in thickness, brightness and morphology. These observations indicate a modified surface appearance relative to the unreinforced alloy. Nevertheless, the apparent changes in feature size and boundary complexity should not be interpreted directly as evidence of grain refinement or a more uniform reinforcement distribution. Such conclusions would require consistently acquired images and quantitative measurements supported by reliable feature identification.

The SEM micrograph of Sample 4A, containing 8 wt.% CSA and 10 wt.% BronzoChrom 10185, is shown in Figure 2(e). It exhibits a dense network of bright, irregular features surrounding numerous dark regions, resulting in a comparatively intricate surface morphology. Localized clustering and void-like features may be present, but their identities and extent cannot be confirmed from the image alone. If verified as reinforcement agglomerates or pores, these features could indicate local heterogeneity in the composite microstructure. Such heterogeneity may influence

mechanical behaviour by producing non-uniform deformation or local stress concentrations; however, the actual contribution of these features to the measured tensile strength, hardness and elongation cannot be established from the SEM image alone.

To complement the qualitative observations, preliminary grayscale image segmentation was used to estimate the apparent area fraction occupied by relatively dark features in each micrograph. The estimated values were 24.6%, 42.5%, 25.1%, 31.9% and 43.7% for Samples 0A, 1A, 2A, 3A and 4A, respectively. The results show a non-monotonic variation in the apparent dark-feature area fraction, with the highest estimates occurring in Samples 1A and 4A and lower values in Samples 0A and 2A. This variation indicates that the relative prevalence of dark regions differs among the examined images. However, the measured fractions are image-segmentation descriptors rather than validated measurements of reinforcement content or porosity. The dark features have not been independently identified, and differences in image contrast and acquisition conditions may influence the segmentation results. Consequently, these percentages should be interpreted as preliminary comparative measurements rather than definitive physical properties of the composites.

Overall, the SEM micrographs demonstrate differences in surface morphology between unreinforced AA6061 and the hybrid composites containing CSA and BronzoChrom 10185. The changes are accompanied by variations in the apparent distribution of bright and dark features, with particularly intricate morphologies observed in Samples 1A and 4A.

3.3 Mechanical Properties and Strengthening Mechanism

Tables 4 and 5 show the tensile and Vickers microhardness values of AA6061 hybrid composites. As the total concentration of BronzoChrom 10185 and CSA rose in the examined formulations, the UTS and hardness increased gradually, while the elongation dropped. The simultaneous rise of CSA and BronzoChrom 10185 yields a combined reinforcement system, and the results describe the response of the combined system and not the independent contribution of each reinforcement.

The UTS increased from 118.45 MPa for 0A to 123.82, 129.67, 136.53 and 143.92 MPa for Samples 1A–4A, respectively (Figure 3). Sample 4A showed the greatest UTS, which is 21.50% higher than that of unreinforced AA6061. The observed increase is consistent with possible contributions from an enhanced reinforcing population, resistance to plastic deformation, particle–dislocation interactions and interfacial load transmission. A prerequisite for load transfer from the aluminium matrix to relatively hard reinforcement particles, which is a well-established strengthening process in particulate metal matrix composites, is effective particle–matrix interaction [18]. More generally, particulate reinforcements can contribute to strengthening through particle–matrix load transfer and interactions with dislocations, while reinforcement distribution, particle–matrix compatibility and particle clustering can influence the effectiveness of these mechanisms [19]. Similar enhancements in mechanical properties have been documented for nickel-containing aluminium composites [14], [15]. Liu [20] noted that the mechanical response of NiBSi-containing composites is contingent on reinforcement features and microstructural evolution, although a different matrix system was employed.

The oxide-rich CSA comprises considerable quantities of SiO_2 and other metal oxides, which can provide dispersed particles that impede plastic deformation and restrict dislocation migration. Tejyan [9] also found that the tensile strength and hardness of AA6061 were improved with the addition of CSA. More generally, distributed reinforcing particles can strengthen aluminium matrices by hindering dislocation mobility and plastic deformation [21]. In the present work, these mechanisms are treated as feasible interpretations of the observed mechanical trend rather than independently established strengthening contributions.

The elongation dropped from 39.67% for 0A to 27.90% for 4A, representing a reduction of 29.67% (Figure 4). This decrease is consistent with the expected trade-off between strength and ductility associated with increasing particle reinforcement. Localized particle clustering and micro-porosity identified in 4A may also have served as locations for stress concentration and premature damage onset, contributing to the decreased elongation.

The Vickers hardness increased gradually from 61.8 ± 1.29 HV for 0A to 75.8 ± 1.29 HV for 4A (Figure 5). Thus, 4A recorded the largest gain of 22.65%. The progressive rise is associated with the increasing amount of relatively hard reinforcement in the examined compositions and the observed changes in particle population and distribution.

The observed strengthening is presumably related to reinforcement dispersion, matrix–particle load transfer and constrained dislocation motion; however, these mechanisms were not assessed individually. Thus, the present data do not allow experimental confirmation of the strengthening contributions from Hall–Petch, Orowan or thermal-expansion-mismatch mechanisms. Furthermore, while CSA and BronzoChrom 10185 were altered concurrently, the

current findings cannot attribute a specific contribution to each reinforcement or prove a synergistic strengthening effect.

Table 4: Tensile properties of AA6061/Ni–B-Si powder/CSA hybrid composites

Sample	CSA (wt.%)	Ni–B–Si (wt.%)	UTS (MPa)	UTS change vs. 0A	Elongation (%)	Elongation change vs. 0A
0A (Control)	0	0	118.45	—	39.67	—
1A	2	2	123.82	+4.53%	36.80	−7.23%
2A	4	6	129.67	+9.48%	33.90	−14.54%
3A	6	8	136.53	+15.26%	30.80	−22.36%
4A	8	10	143.92	+21.50%	27.90	−29.67%

Note: UTS = ultimate tensile strength; CSA = coconut shell ash.

Table 5: Vickers microhardness of AA6061/Ni–B–Si powder/CSA hybrid composites

Sample	Ni–B–Si powder (wt.%)	CSA (wt.%)	Indentation 1 (HV)	Indentation 2 (HV)	Indentation 3 (HV)	Indentation 4 (HV)	Mean ± SD (HV)
0A	0	0	60.3	61.3	62.3	63.3	61.8 ± 1.29
1A	2	2	63.1	64.1	65.1	66.1	64.6 ± 1.29
2A	6	4	68.4	69.4	70.4	71.4	69.9 ± 1.29
3A	8	6	70.5	71.5	72.5	73.5	72.0 ± 1.29
4A	10	8	74.3	75.3	76.3	77.3	75.8 ± 1.29

Note: HV = Vickers hardness; SD = sample standard deviation; n = 4 indentation measurements per specimen.

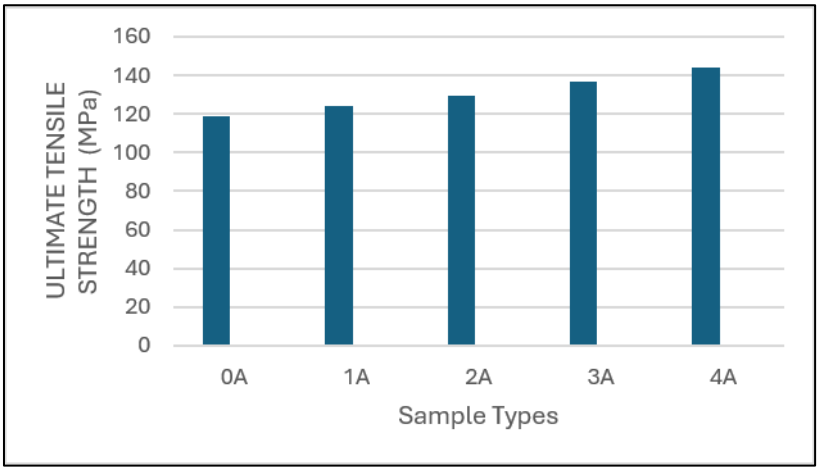


Figure 3: Ultimate Tensile Strength of the AA6061 Control Alloy and Hybrid-Reinforced Composites

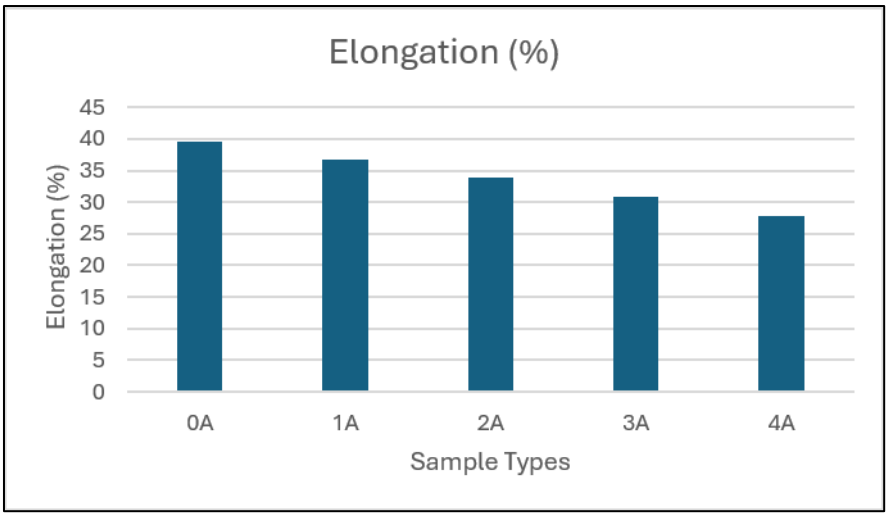


Figure. 4: Elongation of the AA6061 Control Alloy and Hybrid-Reinforced Composites

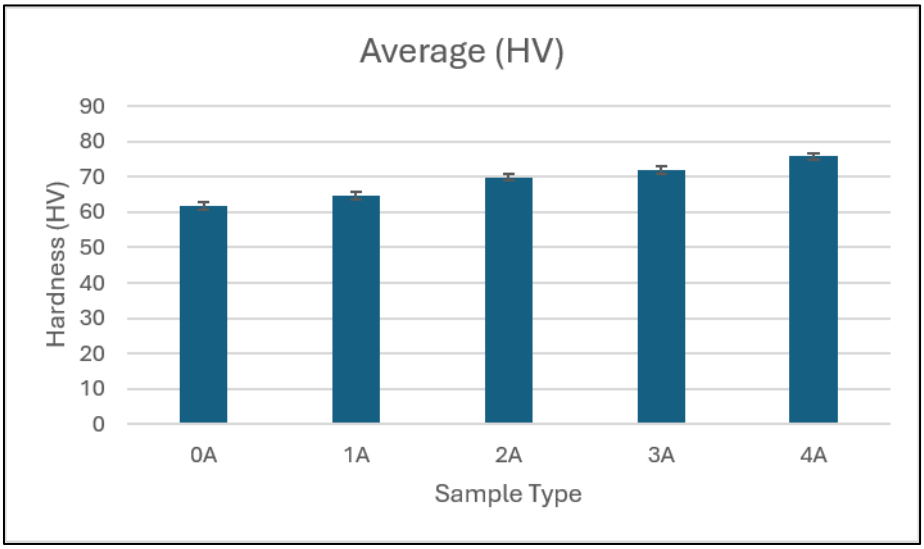


Figure 5: Vickers Microhardness of the AA6061 Control Alloy and Hybrid-Reinforced Composites

3.4 Microstructure–Mechanical Property Correlation

The combined SEM observations and mechanical test results reveal a consistent relationship between increasing reinforcement content and the mechanical response of the AA6061 matrix. The SEM micrographs indicate an increasing presence of reinforcing particles, with generally satisfactory particle distribution and apparent contact between the particles and the surrounding matrix. These microstructural characteristics provide a plausible explanation for the progressive increases in ultimate tensile strength (UTS) and Vickers hardness observed from sample 0A to 4A.

The increase in UTS from 118.45 MPa to 143.92 MPa and hardness from 61.8 HV to 75.8 HV is consistent with the contribution of hard reinforcing particles to resistance against plastic deformation. The particles may enhance load transfer, impede dislocation movement, and restrict localized plastic deformation within the aluminium matrix [9], [18], [21]. The effectiveness of these mechanisms depends on factors such as particle distribution, particle–matrix interfacial contact, and interactions between the reinforcing particles and dislocations. Conversely, particle clustering may reduce the effectiveness of reinforcement and promote localized stress concentrations [19]. Previous studies have similarly emphasized the importance of reinforcement distribution and particle–matrix interaction in determining the mechanical performance of aluminium-based composites [22]. Furthermore, the mechanical response of Ni–B–Si-containing composites may depend on reinforcement characteristics and the resulting microstructural development [12], [15], [20].

At the highest reinforcement level (sample 4A), the maximum UTS and hardness were accompanied by localized particle clustering and increased micro-porosity. Although the higher reinforcement content contributed to improved strength and hardness, these microstructural imperfections may have introduced localized stress concentrations and facilitated

crack initiation during tensile deformation. Such effects could partly explain the reduction in ductility observed at the highest reinforcement level. These interpretations are consistent with previous reports highlighting the influence of reinforcement distribution, interfacial characteristics, and microstructural heterogeneity on the deformation behaviour of aluminium matrix composites [9], [18], [23]. However, the individual contributions of particle clustering and micro-porosity to the observed mechanical response cannot be established from the available observations alone.

The quantitative comparison presented in Table 6 further demonstrates the relationship between reinforcement content and mechanical performance. Within the investigated composition range, UTS and hardness increased progressively, whereas elongation decreased, indicating a strength–ductility trade-off. Sample 4A exhibited the largest improvements in UTS and hardness relative to unreinforced AA6061, with increases of 21.50% and 22.65%, respectively. However, these improvements were accompanied by a 29.67% reduction in elongation. This behaviour suggests that increasing the combined reinforcement content enhanced resistance to plastic deformation but reduced the capacity of the composite to undergo tensile deformation before fracture.

Table 6: Percentage change in mechanical properties relative to unreinforced AA6061

Sample	Ni–B–Si alloy (wt.%)	CSA (wt.%)	UTS improvement (%)	Hardness improvement (%)	Elongation reduction (%)
0A	0	0	0.00	0.00	0.00
1A	2	2	4.53	4.53	7.24
2A	6	4	9.47	13.11	14.54
3A	8	6	15.26	16.50	22.36
4A	10	8	21.50	22.65	29.67

Overall, the microstructures observations are consistent with the measured mechanical response. However, the observed improvements should be understood as the reaction of the integrated BronzoChrom 10185-CSA reinforcing system. As both reinforcement contents were increased simultaneously, the present study does not establish the independent contribution of each reinforcement or a conclusive synergistic connection between them.

4 CONCLUSIONS

AA6061 hybrid composites reinforced with Eutalloy® BronzoChrom 10185, a commercial nickel-based Ni–B–Si alloy, and coconut shell ash (CSA) were successfully fabricated by stir casting. SEM observations revealed changes in surface morphology with increasing combined reinforcement content, with localized particle clustering and void-like features evident at the highest reinforcement level.

The measured ultimate tensile strength (UTS) and Vickers hardness increased progressively with increasing combined reinforcement content. Sample 4A, containing 10 wt.% BronzoChrom 10185 and 8 wt.% CSA, achieved the highest UTS of 143.92 MPa and hardness of 75.8 HV, representing increases of 21.50% and 22.65%, respectively, relative to unreinforced AA6061. Conversely, elongation decreased from 39.67% to 27.90%, corresponding to a reduction of 29.67% and indicating a strength–ductility trade-off.

The observed mechanical response may be associated with reinforcement-related load transfer and restricted plastic deformation. However, these mechanisms were not independently verified, and the contributions of Hall–Petch, Orowan and thermal-expansion-mismatch strengthening remain unconfirmed. Furthermore, because the CSA and BronzoChrom 10185 contents were increased simultaneously, the results represent the response of the combined reinforcement system and do not establish the independent effects or a definitive synergistic contribution of either reinforcement. Since only one tensile specimen was tested per composition, the observed trends should also be interpreted cautiously.

Overall, the BronzoChrom 10185–CSA hybrid system showed potential for improving the measured strength and hardness of AA6061 within the investigated composition range, albeit with reduced ductility. Further research involving replicated tensile tests, independent variation of reinforcement contents and quantitative microstructural analysis is required to validate these trends, distinguish the individual reinforcement effects and clarify the underlying strengthening mechanisms.

STATEMENTS ON COMPLIANCE WITH ETHICAL STANDARDS

Acknowledgments

The authors sincerely appreciate the Tertiary Education Trust Fund (TETFund) for funding this research through the Institutional-Based Research (IBR) Grant and the Management of Lagos State University of Science and Technology, Ikorodu, for its institutional support.

Funding Source

Details of funding source must be inserted here.

Disclosure of conflict of interest

The authors declare no conflicts of interest regarding this manuscript.

REFERENCES

[1] Hatti, G., Naveen, G. J., Koti, V., Uppin, V. S., Lingaraju, S. V., Janamatti, S., Hokrani, V. V., & Pujar, S. N. (2024). Green metal matrix composites: A multi-faceted study on Al alloy composites with eggshell powder and silicon carbide as reinforcements. *Metallurgical Research & Technology,* 121(6), 610. https://doi.org/10.1051/metal/2024086

[2] Prabhu, B., Prakash, M., Ramasamy, N., Kanagasabai, V., Mohanraj, T., Vijay, D., & Arunkumar, T. (2025). Cleaner production of performance-enhanced hybrid composites using agro-industrial wastes: A sustainable waste management strategy. *Journal of Environmental Management*, 381, 125116. https://doi.org/10.1016/j.jenvman.2025.125116

[3] Samantra, C., Pradhan, S., Kumari, K., Rana, S. K., & Barua, A. (2026). Fabrication, mechanical characterization, and wear optimization of Al6061-CSAp metal matrix composites using hybrid Taguchi-ARAS-Sunflower Algorithm Approach. Proceedings of the Institution of Mechanical Engineers, Part C: Journal of Mechanical Engineering Science. https://doi.org/10.1177/09544062261432683

[4] Bodunrin, M. O., Alaneme, K. K., & Chown, L. H. (2015). Aluminium matrix hybrid composites: A review of reinforcement philosophies; mechanical, corrosion and tribological characteristics. Journal of Materials Research and Technology, 4(4), 434–445. https://doi.org/10.1016/j.jmrt.2015.05.003

[5] Kumar, R., Shringi, D., & Bairwa, K. N. (2022). Microstructure and mechanical behavior of Al6061/Ni/Cr hybrid nano metal matrix composites with addition of graphene and magnesium. Materials Today: Proceedings, 56, 3544–3549. https://doi.org/10.1016/j.matpr.2021.11.260

[6] Tang, S., Shao, S., Liu, H., Jiang, F., Fu, D., Zhang, H., & Teng, J. (2021). Microstructure and mechanical behaviors of 6061 Al matrix hybrid composites reinforced with SiC and stainless-steel particles. *Materials Science and Engineering:* A, 804, 140732. https://doi.org/10.1016/j.msea.2021.140732

[7] Yekinni, A. A., Bello, S. K., Bajela, G. G., & Adigun, I. A. (2020). Effect of coconut shell ash and graphite particles on microstructure and mechanical properties of recycled aluminium composites. *International Journal of Advances in Scientific Research and Engineering, 6*(10), 61–71. https://doi.org/10.31695/IJASRE.2020.33904

[8] Jaga Kumar, L., Vishwanatha, J. S., Ganjigatti, J. P., Irfan, G., & Thara, R. (2023). Investigation of mechanical properties of Al6061 with reinforcement of coconut shell ash and graphene metal matrix composites. *Materials Today: Proceedings,* 92, 413–417. https://doi.org/10.1016/j.matpr.2023.05.529

[9] Tejyan, S., Tiwari, A. K., Kumar, N., Singh, V., & Gangil, B. (2024). Influence of coconut shell ash and cow dung ash reinforcement on the mechanical properties of aluminum alloy composites synthesized by stir casting. Materials Today: Proceedings. https://doi.org/10.1016/j.matpr.2024.05.099

[10] Jaga Kumar, L., Ganjigatti, J. P., Irfan, G., Thara, R., Aradhya, P. J., Choudhary, R. K., Shrigandhi, G. D., & Gurunagendra, G. R. (2025). Effect of graphene and coconut shell ash on mechanical properties of Al6061 metal matrix composites. Journal of The Institution of Engineers (India): Series D, 106(2), 1043–1051. https://doi.org/10.1007/s40033-024-00708-6

[11] Poornesh, M., Bhat, S., Bellairu, P. K., & McDermott, O. (2024). Enhancement of tensile strength of coconut shell ash reinforced Al-Si alloys: A novel approach to optimize composition and process parameters simultaneously. *Processes,* 12(7), 1521. https://doi.org/10.3390/pr12071521

[12] Kumar, R., & Bairwa, K. N. (2023). Optimizing Al6061-based hybrid metal matrix composites: Unveiling microstructural transformations and enhancing mechanical properties through Ni and Cr reinforcements.

EVERGREEN Joint Journal of Novel Carbon Resource Sciences & Green Asia Strategy, 10(4), 2161–2172. https://doi.org/10.5109/7160891

[13] Beldar, P. R., & Kumavat, H. R. (2024). Comparative analysis of mechanical properties of SiC particle addition on Al6061/Ni and Al6061/Cr metal matrix composites. *Materials Letters, 369*, 136745. https://doi.org/10.1016/j.matlet.2024.136745

[14] Nath OP, A. R., & Arul, S. (2020). Effect of nickel reinforcement on micro hardness and wear resistance of aluminium alloy Al7075. *Materials Today: Proceedings,* 24, 1042–1051. https://doi.org/10.1016/j.matpr.2020.04.418

[15] Syahid, M., & Sina, M. T. I. (2025). Mechanical properties and wear resistance of SiC-reinforced aluminium matrix composite with nickel addition. *Journal of Mechanical Engineering and Sciences,* 19(4), 10832–10844. https://doi.org/10.15282/jmes.19.4.2025.1.0849

[16] Yashpal, Sumankant, Jawalkar, C. S., Verma, A. S., & Suri, N. M. (2017). Fabrication of aluminium metal matrix composites with particulate reinforcement: A review. Materials Today: Proceedings, 4(2), 2927–2936. https://doi.org/10.1016/j.matpr.2017.02.174

[17] Castolin Eutectic. (n.d.). Eutalloy 10185 powder: Technical data sheet**.** Castolin Eutectic.

[18] Maurya, P., Kota, N., Gibmeier, J., Wanner, A., & Roy, S. (2022). Review on study of internal load transfer in metal matrix composites using diffraction techniques. *Materials Science and Engineering: A, 840*, 142973. https://doi.org/10.1016/j.msea.2022.142973

[19] Geng, R., Qiu, F., & Jiang, Q.-C. (2018). Reinforcement in Al matrix composites: A review of strengthening behavior of nano-sized particles. Advanced Engineering Materials, **20**(9), 1701089. https://doi.org/10.1002/adem.201701089

[20] Liu, C., Peng, H., Zhao, Y., et al. (2019). Microstructure, mechanical and corrosion properties of electron-beam-melted and plasma-transferred arc-welded WC_p/NiBSi metal matrix composites. Rare Metals. https://doi.org/10.1007/s12598-018-1096-9

[21] Farid, W., Luo, K.-G., Kong, C., & Yu, H.-L. (2026). Advancements in accumulative roll bonding based process for developing aluminum matrix composites reinforced with particles: A review. *Transactions of Nonferrous Metals Society of China, 36*(8), 2205–2232. https://doi.org/10.1016/S1003-6326(26)67089-6

[22] Ashebir, D. A., Mengesha, G. A., & Sinha, D. K. (2022). An insight into mechanical and Qmetallurgical behavior of hybrid reinforced aluminum metal matrix composite. Advances in Materials Science and Engineering, 2022**,** Article 7843981. https://doi.org/10.1155/2022/7843981

[23] Saiyathibrahim, A., Jatti, V. S., Dhanapal, P., & Mohan, D. G. (2024). Development and characterization of in-situ nickel aluminide reinforced Al-Si matrix composites by stir casting. *Engineering Reports, 6*(12), e12966. https://doi.org/10.1002/eng2.12966.